



# Simulation and Optimization of a Three-Level Inverter Driven Induction Motor System

Weijie Chu<sup>1</sup> and Siyu Yu<sup>2,\*</sup>

<sup>1</sup> School of Electrical Engineering, Shanghai University of Electric Power, 2588 Changyang Road, Yangpu District, Shanghai 200090, China

<sup>2</sup> College of Mechanical Engineering, Northern Arizona university, S San Francisco St, Flagstaff, AZ 86011, USA

\*sy556@nau.edu

**Abstract.** In high-performance induction motor applications, multilevel inverters have demonstrated the capability to deliver cleaner voltage waveforms than conventional topologies. Nevertheless, their implementation can be hampered by issues such as circuit complexity, neutral-point voltage imbalance, and substantial switching losses. This work develops a unified optimization framework that merges an improved Space Vector Pulse Width Modulation (SVPWM) technique, a resonant soft-switching stage, and silicon carbide (SiC) power devices. Within this approach, capacitor voltage balance is actively regulated using a strategy derived from the  $d-q$  model of a neutral-point-clamped (NPC) three-level inverter coupled to an induction motor. Soft switching is enabled via an auxiliary resonant circuit to achieve Zero-Voltage Switching (ZVS), while SiC devices help to lower both switching and conduction losses. Simulation results reveal that the proposed scheme achieves a total harmonic distortion (THD) below 3.5%, a load-disturbance recovery time of 0.12 s, torque ripple under 5%, and a 28% decrease in switching losses, which improves efficiency from 93.2% to 96.1%. Voltage deviation across capacitors remains within  $\pm 4\%$ , confirming the reliability and potential industrial relevance of this design.

**Keywords:** Space Vector Pulse Width Modulation (SVPWM), Silicon Carbide (SiC) Power Devices, Capacitor Voltage Balance, Three-Level Inverter, Zero-Voltage Switching (ZVS).

## 1 Introduction

With the rapid development of industrial automation, electric vehicles and intelligent manufacturing, the demand for high-performance and efficient motor drive systems has been steadily increasing. Induction motors are widely used in manufacturing plants and processing industries due to their mechanical robustness, moderate maintenance requirements and cost-effectiveness.

In recent years, multilevel inverter technology has become increasingly popular for high-performance induction motor drives due to its capability to improve output voltage

waveforms, reduce harmonic distortion, and mitigate  $dv/dt$  stress. Among various topologies, the Neutral Point Clamped (NPC) three-level inverter is widely adopted for its symmetrical structure and scalability. Previous investigations, such as the work by Shukla et al., have shown that NPC inverters can generate nearly sinusoidal voltages with relatively low harmonic distortion. Nevertheless, challenges such as capacitor voltage balancing and switching loss reduction remain areas for further improvement [1].

In international research, Zhang et al. proposed an improved SVPWM method that significantly reduces voltage imbalance and harmonic distortion [2]. Chen et al. attempted to introduce silicon carbide (SiC) devices into multilevel inverters, achieving higher efficiency and reduced losses through hybrid device layouts [3]. Rodriguez et al. reviewed topological and control advancements aimed at neutral-point stabilization [4]. Domestically, related studies have largely focused on single control strategies or specific structural optimizations, with relatively limited research on systematic optimization through multi-technology integration.

In response, this paper presents a coordinated optimization method implemented in PLECS, combining enhanced SVPWM, real-time capacitor voltage balancing, ZVS-based soft switching, and SiC devices. The proposed framework is assessed in terms of waveform quality, transient response, efficiency, and voltage balance, under both steady-state operation and sudden load variations.

## 2 System modeling

### 2.1 Neutral-point-clamped three-level inverter topology

The three-phase NPC topology used here is shown in Fig.1. Each phase consists of four switching devices and two DC-side capacitors, with the midpoint capacitor providing the basis for voltage balancing.

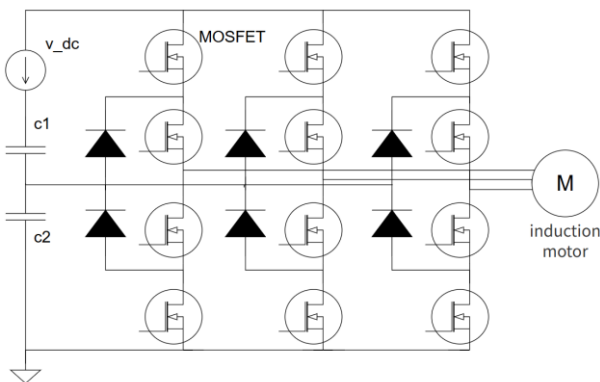


Fig. 1. Schematic diagram of the topology

The output voltage of the inverter has three levels:

$$V_{out} \in \left\{ +\frac{V_{dc}}{2}, 0, -\frac{V_{dc}}{2} \right\} \quad (1)$$

Where  $V_{dc}$  represents the overall value of the voltage on the DC side.

## 2.2 Induction Motor d-q Coordinate System Model

To simplify the dynamic analysis of the motor, a synchronous rotating coordinate system (d-q axis) model is used, and the voltage equation is shown in Equation (2):

$$\begin{cases} V_{dd} = R_s I_{dd} + \frac{d\psi_{dd}}{dt} - \omega_e \psi_{qd} \\ V_{qd} = R_s I_{qd} + \frac{d\psi_{qd}}{dt} - \omega_e \psi_{dd} \\ 0 = R_r I_{dz} + \frac{d\psi_{dz}}{dt} - (\omega_e - \omega_r) \psi_{qz} \\ 0 = R_r I_{qz} + \frac{d\psi_{qz}}{dt} + (\omega_e - \omega_r) \psi_{dz} \end{cases} \quad (2)$$

Where  $V_{dd}, V_{qd}$  represent the d-axis and q-axis components of the stator voltage;  $I_{dd}, I_{qd}, I_{dz}, I_{qz}$  represent current components for both stator and rotor;  $R_s, R_r$  represent the stator and rotor resistances;  $\psi_{dd}, \psi_{qd}, \psi_{dz}, \psi_{qz}$  represent flux components of the stator and rotor;  $\omega_e$  represents the electrical angular velocity;  $\omega_r$  represents the rotor mechanical angular velocity.

The torque expression is shown in Equation (3):

$$T_e = \frac{3}{2} p (\psi_{dd} I_{qd} - \psi_{qd} I_{dd}) \quad (3)$$

Where  $p$  represents the quantity of pole pairs.

Parameter settings are based on typical industrial induction motors, as listed in Table 1.

**Table 1.** Main Parameter Settings of Induction Motor and Inverter.

Parameter name	Value	Description
Rated Power $P_{rated}$	7.5 kW	Three-Phase Induction Motor for Industrial Applications
Rated Voltage $V_{rated}$	380 V	Three-Phase AC Input
Number of Pole Pairs $p$	2	-
Rated Frequency $f$	50 Hz	-
Stator Resistance $R_s$	0.435 $\Omega$	-
Rotor Resistance $R_r$	0.816 $\Omega$	-
Stator Inductance $L_s$	2.0 mH	-

Rotor Inductance $L_r$	2.0 mH	-
Mutual Inductance $L_m$	69.31 mH	-
DC Bus Voltage $V_{dc}$	600 V	Total DC-Side Voltage of NPC Three-Level Converter
Capacitor Target Voltage $V_{c,ref}$	300 V	Ideal Voltage of Each Neutral- Point Capacitor
Inverter Switching Frequency	10 kHz	-
Zero Voltage Switching (ZVS)	100 kHz	Used for Soft-Switching Design
SiC Switching Device Models (Example)	C3M0032120K	WolfSpeed, 1200V, 32A

### 3 Control Strategy Design

#### 3.1 Improved Space Vector PWM Algorithm

Traditional SVPWM controls the inverter output voltage by selecting from eight effective vector combinations. The conventional SVPWM algorithm achieves control of the inverter output voltage by choosing different combinations of eight effective voltage vectors. This paper designs an improved SVPWM algorithm that draws on the ideas of vector division and switch sequence optimization to effectively suppress midpoint voltage oscillation and reduce harmonic distortion in the output voltage [5]. The specific steps of the improved algorithm are as follows:

1) Determine the sector where the reference voltage vector is located

a. Calculate the phase angle of the reference voltage vector:

$$\theta = a \tan 2(V_{ref_y}, V_{ref_x}) \quad (4)$$

Where  $a \tan 2(y, x)$  represents the vector whose direction is calculated using the arctangent function;  $V_{ref_y}$  and  $V_{ref_x}$  represent the components of the reference voltage vector along  $\beta$ -axis and  $\alpha$ -axis, respectively.

b. Determine the sector  $S$  in which  $V_{ref}$  is located based on the phase angle  $\theta$ . Each sector spans an angle of  $\Pi/3$ , so the sector can be expressed as shown in Equation (5), with the corresponding sector numbers being 0, 1, 2, 3, 4, and 5.

$$S = \left[ \frac{3}{\Pi} \cdot \theta \right] \quad (5)$$

c. Once the sector is determined, the subsequent steps will be based on the valid vector combinations within that sector.

2) Calculate the duty cycle ratio of the two adjacent basis vectors

Once the sector containing the reference voltage vector has been identified, two adjacent base vectors  $\vec{v}_1$  and  $\vec{v}_2$  within that sector are selected. The corresponding duty cycles  $D_1$  and  $D_2$  of these base vectors are then calculated, ensuring that their sum equals

The specific steps are as follows:

a. Calculate the duty cycles based on the geometric relationship between the reference voltage vector  $\vec{V}_{ref}$  and the base vectors  $\vec{V}_1$  and  $\vec{V}_2$ . First, compute the resultant vector formed by  $\vec{V}_1$  and  $\vec{V}_2$ :

$$\vec{V}_{ref} = D_1 \vec{V}_1 + D_2 \vec{V}_2 \quad (6)$$

Where  $D_1$  and  $D_2$  are the duty cycles of the basis vectors  $\vec{V}_1$  and  $\vec{V}_2$  respectively.

b. Based on the geometric relationship, the calculation formulas for  $D_1$  and  $D_2$  are as follows:

$$D_1 = \frac{|\vec{V}_{ref}| \cdot \sin(\theta - \alpha)}{|\vec{V}_1| \cdot \sin \beta} \quad (7)$$

$$D_2 = 1 - D_1 \quad (8)$$

c. Once  $D_1$  and  $D_2$  are calculated, the duty cycles of the two base vectors can be determined.

### 3) Zero vector selection and capacitor voltage balancing

When a high or low capacitor voltage is detected, the control system prioritizes selecting the zero vector that helps balance the voltage and adjusts its duration accordingly, thereby gradually correcting the neutral-point voltage. This method enhances response sensitivity and regulation capability, effectively mitigating the fluctuations caused by voltage imbalance [6].

4) Real-time adjustment of switch sequence and control of capacitor voltage deviation

The control system adopts a feedback-based regulation method, using the voltage deviation as an input signal to correct the duty cycle of zero vectors and the allocation logic of the switching sequence. Without increasing the system complexity, this approach enhances the inverter's voltage control capability under dynamic conditions and helps reduce torque disturbances caused by midpoint drift.

## 3.2 Capacitor Voltage Balancing Control Logic

This paper adopts a feedback regulation-based capacitor voltage balancing control method to achieve dynamic balance of multiple capacitor voltages [6]. The capacitor balancing control logic designed in this paper is based on the feedback regulation principle, aiming to adjust the capacitor voltages in real-time and maintain their balance.

The capacitor voltage balancing control method monitors the deviation between the actual voltage of each capacitor and the set target voltage, dynamically adjusting the frequency of zero vector usage frequency and accordingly adjust the duty cycle to stabilize the voltage balance of the capacitor. Its control rate is shown in Equation (9):

$$u_{eq} = K_p (V_{c,ref} - V_c) + K_i \int (V_{c,ref} - V_c) dt \quad (9)$$

Where  $V_{c,ref} = V_{dc} / 2$ ,  $V_c$  is the actual capacitor voltage.

## 4 Simulation Design and Results

### 4.1 Formatting the title, authors and affiliation

The system is primarily composed of the following modules:

- **Three-Level Inverter Module:** This module employs SiC MOSFETs as switching devices and integrates an improved SVPWM control strategy to generate appropriate voltage vectors.

- **Induction Motor Module:** Utilizes a d-q coordinate system model to simulate the motor's voltage, current, and torque characteristics under dynamic operating conditions.

- **Control Module:** Incorporates the SVPWM control algorithm, capacitor voltage balancing logic, and the design of an auxiliary resonant circuit to enable soft-switching (ZVS).

- **Feedback Module:** Continuously monitors the motor's operating state and the capacitor voltages. It adjusts the system's operational behavior through real-time feedback to ensure voltage balance and stable performance.

The detailed system block diagram is shown in Fig. 2 below:

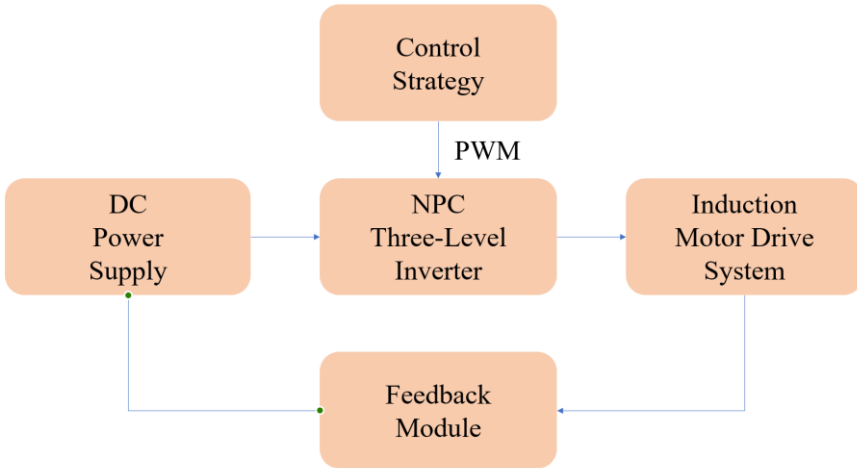


Fig. 2. Simulation Model System Block Diagram.

The main parameters are listed in Table 2.

**Table 2.** System Parameters.

Parameter	Value	Note
DC Voltage $V_{dc}$	600 V	-
Rated Motor Power	7.5 kW	-
Number of Pole Pairs $p$	2	-
Rated Capacitor Voltage	300 V	Per capacitor
Inverter Switching Frequency	10 kHz	-
Soft-Switching Resonant Frequency	100 kHz	-
SVPWM Vector Update Period	100 $\mu$ s	Controller refresh rate
Simulation Step Size	1 $\mu$ s	Suitable for PLECS accuracy
Total Simulation Time	1 s	Used for stability testing

In the simulation, an auxiliary resonant circuit and SiC MOSFET devices are introduced. The former achieves Zero Voltage Switching (ZVS) at the switching instant through the resonance between inductance and capacitance, effectively reducing switching losses and electromagnetic interference (EMI) [7]. The latter, due to its low conduction loss and high switching temperature characteristics, accelerates the dynamic response of the system and improves operational efficiency.

## 4.2 Output waveform and harmonics analysis

Fig. 3 respectively shows the line voltage waveform of the three-level inverter and the single-phase spectral analysis diagram. It can be seen from Fig.3 (a) that the line voltage waveform is generally a relatively smooth ideal sine wave. Fig.3 (b) shows the spectrum diagram of FFT analysis on one of the three phases, and it can be seen that the harmonic content is close to zero. Through subsequent calculations, it can be concluded that the total harmonic distortion (THD) can be controlled below 3.5%, which is significantly lower than the 7%-10% of traditional two-level inverters, reducing the overall energy loss of the system.

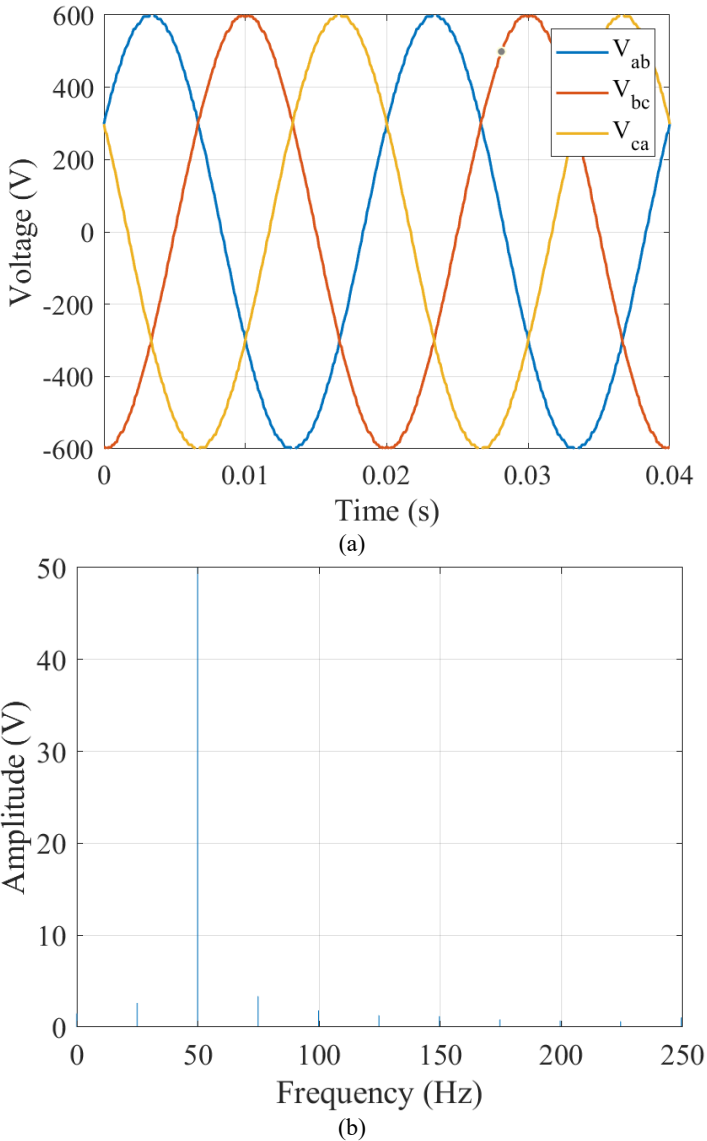


**Fig. 3.** line voltage waveform of the Three-level Inverter: (a) Inverter Output Line Voltage Waveform; (b) The voltage spectrum diagram of the  $V_{ab}$ .

### 4.3 Dynamic response performance

Fig.4 respectively shows the load torque curves and the rotor speed response under step load disturbance. As can be seen from Fig.4 (a), the rotor speed has undergone a process of slowly decreasing from 0.4pu to 0.3pu and then rapidly recovering and rising back to 0.4pu. It can be concluded that the overall robustness of the system is relatively good. As can be seen from Fig.4 (b), the process in which the load rapidly drops from 0.8Nm

to 0.4Nm and then quickly recovers to 0.55 can also reflect the overall robustness of the system, enabling it to make extremely rapid adjustments when disturbed.

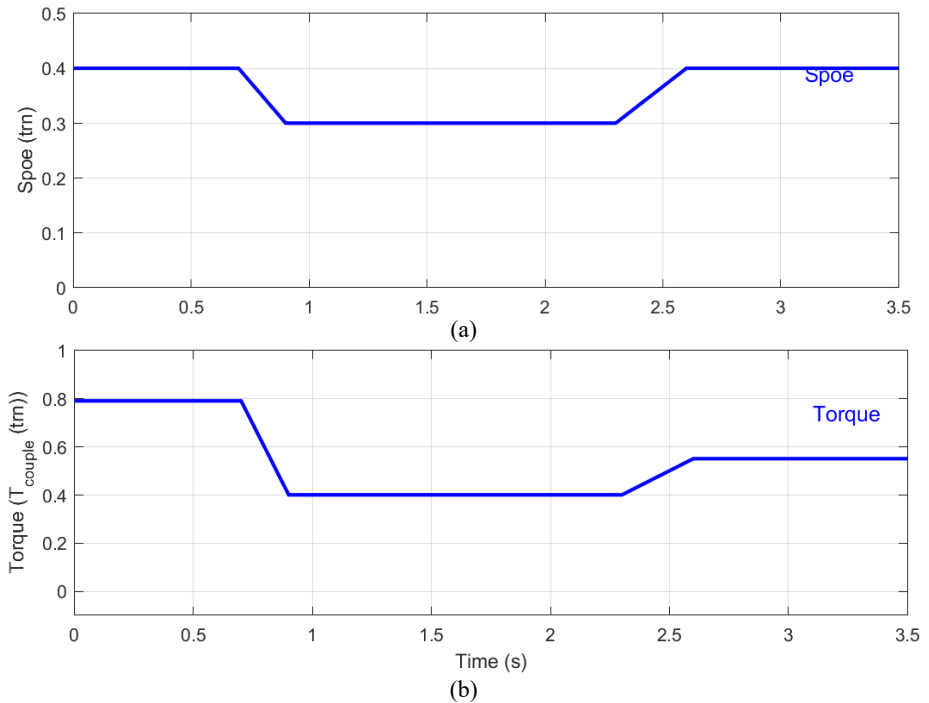


**Fig. 4.** dynamic response performance: (a) Load torque curve under step load disturbance; (b) Rotor speed response under step load disturbance.

#### 4.4 Capacitor voltage balancing performance

Fig. 5 shows the capacitor voltage waveform. Through calculation, it can be concluded that the voltage deviation of the two capacitors always remains within  $\pm 4\%$  or less, thereby demonstrating the effectiveness of the capacitor voltage balancing control strategy. It effectively suppresses voltage fluctuations and thus enhances the stability and reliability of the system operation.

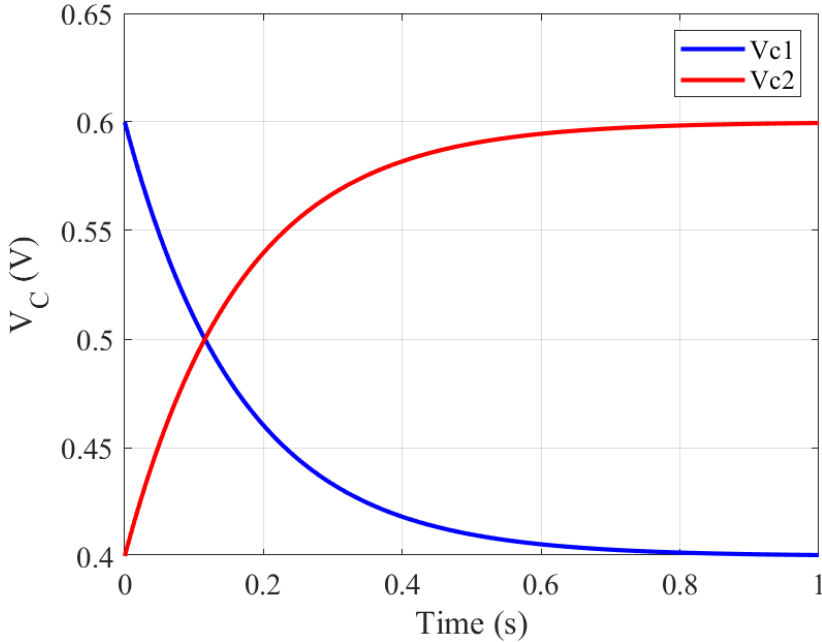


Fig. 5. Capacitor Voltage Waveform.

#### 4.5 Switching losses and system efficiency

After implementing soft-switching technology and SiC devices, the system's switching losses dropped by around 28%, raising efficiency from 93.2% to 96.1%. This improvement not only saves energy but also eases the system's thermal management. In conventional silicon-based devices, high switching losses produce significant heat, requiring complicated cooling solutions, whereas soft-switching reduces losses by carefully timing the switching operations [8].

Using SiC devices further improves thermal handling and switching efficiency. Their ability to operate at higher temperatures and lower conduction resistance allows higher-frequency operation with less loss [9]. Overall, combining soft-switching with SiC devices boosts efficiency, reduces thermal stress, extends device lifespan, and ensures more reliable long-term operation [10].

## 5 Conclusion

This paper presents a comprehensive optimization scheme for a NPC three-level inverter driving an induction motor. The approach integrates an improved SVPWM algorithm, capacitor voltage balancing, a soft-switching assisted resonant circuit, and SiC power devices, achieving coordinated multi-objective improvements in output voltage quality, dynamic response, switching losses, and overall efficiency. A complete control system simulation model was built on the PLECS platform, and quantitative analysis of key parameters confirmed the scheme's effectiveness. Step disturbance

simulations further showed rapid speed recovery within 0.12 seconds and high-efficiency operation, with system efficiency reaching 96.1%, demonstrating strong potential for practical engineering applications.

**Authors Contribution.** All the authors contributed equally and their names were listed in alphabetical order.

## References

1. Wang, X., Xiao, H., Ren, Y., Cheng, M.: A novel modulation strategy for split-inductor active NPC inverter with loss distribution balancing and thermal stress reduction. *IEEE Transactions on Power Electronics* 38(6), 7296-7307 (2023).
2. Zhang, L., Fang, X., Tang, Y., et al.: An improved SVPWM algorithm for three-level NPC inverter to reduce neutral-point voltage oscillation. *IEEE Transactions on Power Electronics* 37(1), 856–867 (2022).
3. Chen, Y., Ge, B., Lei, Q., et al.: A high-efficiency three-level inverter with hybrid Si/SiC devices for industrial applications. *IEEE Transactions on Industrial Electronics* 69(5), 4590–4600 (2022).
4. Rodríguez, J., Lai, J.-S., Peng, F.Z.: Multilevel inverters: a survey of topologies, controls, and applications. *IEEE Transactions on Industrial Electronics* 49(4), 724–738 (2002).
5. Tuluhong, A., Song, T., Chang, Q., Xu, Z.: A review of neutral point voltage balancing and common mode voltage suppression methods in three level converters. *Electronics* 14(5), 856-860 (2025).
6. Chen, Z., Liu, J., Zheng, Z.: Neutral point voltage balancing control based on adjusting application times of redundant vectors for three-Level NPC inverter. *IEEE Journal of Emerging and Selected Topics in Power Electronics* 8(1), 714–725 (2020).
7. Wu, Q., Fan, X., Wang, Q.: An improved hybrid ZVS modulation for SiC high frequency three phase inverter. *IEEE Journal of Emerging and Selected Topics in Power Electronics*, early access (2025).
8. Harasimeczuk, M., Kopacz, R., Trochimiuk, P., Miśkiewicz, R., Rąbkowski, J.: Experimental investigation on SiC MOSFET turn-off power loss reduction using the current sink capacitor technique. *Energies* 17(1), 12-13 (2024).
9. Rasul, A., Teixeira, R., Baptista, J.: Silicon carbide converter design: A review. *Energies* 18(8), 14-15 (2025).
10. Mu, X., Wu, W., Blaabjerg, F., et al.: A review of hybrid three level ANPC inverters: topologies, comparison, challenges and improvements in applications. *Energies* 18(10), 22-23 (2025).

**Open Access** This chapter is licensed under the terms of the Creative Commons Attribution-NonCommercial 4.0 International License (<http://creativecommons.org/licenses/by-nc/4.0/>), which permits any noncommercial use, sharing, adaptation, distribution and reproduction in any medium or format, as long as you give appropriate credit to the original author(s) and the source, provide a link to the Creative Commons license and indicate if changes were made.

The images or other third party material in this chapter are included in the chapter's Creative Commons license, unless indicated otherwise in a credit line to the material. If material is not included in the chapter's Creative Commons license and your intended use is not permitted by statutory regulation or exceeds the permitted use, you will need to obtain permission directly from the copyright holder.

